Materials Today Communications 26 (2021) 101980

Contents lists available at ScienceDirect

Materials Today Communications

journal homepage: www.elsevier.com/locate/mtcomm

Evaluation of the fractal dimension of polyacrylamide during gelation and swelling

Ertan Arda [a], Selim Kara [a], Önder Pekcan [b], Gülşen Akın Evingür [c,*]

[a] Department of Physics, Faculty of Science, Trakya University, Edirne, Turkey
[b] Faculty of Engineering and Natural Sciences, Kadir Has University, İstanbul, Turkey
[c] Department of Industrial Engineering, Faculty of Engineering, Pîrî Reis University, Tuzla, İstanbul, Turkey

ARTICLE INFO

Keywords:
Fractal dimension
Polyacrylamide gel
Photon transmission technique
Gelation
Swelling

ABSTRACT

The photon scattering method was performed to monitor the free radical crosslinking copolymerization (FCC) of acrylamide (AAm) applied with N,N′-methylenebis (acrylamide) (Bis) in time. FCC experiments were conducted using different Bis contents to create fractal-like network structures in polyacrylamide (PAAm) gels. Higher intensity values of the scattered photons, I_{sc} were observed with increasing Bis content, *BC*, at a given time, which was attributed to fractal-like macrogel formation from interconnected microgels. The same gels were used in swelling experiments after drying, and increased I_{sc} intensities from the PAAm gels were observed during the swelling process. Fractal dimensions, *d* during the gelation and swelling processes were measured and found to be increased as gelation and swelling times increased. According to the results obtained from the gelation measurements, it was seen that the fractal size, *d*, increased from very small values to 3.00. A similar increase in the range 1.00–1.66 was observed during swelling experiments.

1. Introduction

As known, the interface between a solid and its liquid surroundings may form a fractal-like object with a dimension *d*, in various shapes such as surface, mass and pore-like structures [1]. It has also been well understood that the network structure determines the behavior of polymeric gels with their fractal-like heterogeneities. A non-uniform concentration makes these gels swell to create such heterogeneities. It is known that, in the case of crosslinking of a polymer in a solution, the distribution of the junction points possesses fluctuations in crosslinking density. These swollen gels may possess fractal-like imperfections in polymeric systems. Photon scattering experiments in polymeric gels confirm this behavior for two junctions called “frozen blobs” positioned on adjacent lattice sites [2]. Chemical tight bonding from chain segments sticks together the cross links of the gels that are swollen. Typically, at first, topological neighbors form in the cluster due to these connected frozen blobs. Therefore, a site percolation might appear for polymer chains which are randomly cross-linked on a blob web.

It is evident from the turbid gel that the method of light scattering demonstrates the phase separation regime in which the polymeric solution has two gel phases with different concentrations. The light wavelength for both phases can form a spectrum to inform us of the gelation condition. The strong opacity observed on the gel indicates higher dispersion of light [3]. How intensely light is scattered onto surface and mass fractal objects is closely associated with their current fractal situation [4,5]. Furthermore, the fractal dimension of the initial cluster in the poly (methyl methacrylate) gel can be estimated using the Fluorescence spectroscopic method [6]; the estimate was 2.5 in the literature. More recently, studies on gels with fractal structures have been reported, where the confocal laser scanning microscopy, centrifuge and rheological methods have been used [7–9].

For examination of flaxseed gum gels in terms of rheological properties and fractal dimensions, a variety of ionic strength values is applied (0 −1000 mM). It was reported that these fractal dimensions were computed between 2.06 and 2.49 or 1.42 and 2.18 with different models and ranges of ionic strength [7]. Furthermore, studies on acid (gluconolactone)-induced soy protein isolate gels have been performed with regard to their viscoelastic property and scaling behavior within the range of 0–800 mM. The methods of rheological analysis and confocal laser scanning microscopy approximately identified the fractal dimensions as 2.319–2.729 [8]. The gels of extracellular polymeric substances (EPS) (lightly bound: LB and tightly bound: TB) were examined with pre- and post-measurements of their extraction from sludge using an activation technique to remove gel-like, fractal structures. In this

* Corresponding author.

https://doi.org/10.1016/j.mtcomm.2020.101980
Received 14 July 2020; Received in revised form 13 December 2020; Accepted 15 December 2020
Available online 17 December 2020

regard, the *d*values were estimated as 2.74 for slime, 2.10 for LB-EPS and 2.86 for TB-EPS. Accordingly, TB-EPS ranked first ahead of slime in terms of compatibility and density [9]. More recent studies have investigated basil seed gum (BSG) cross-linking with sodium trimetaphosphate for its fractal structure in the scaling model, based on measurements from rheological analysis with oscillation in low amplitude and shearing so that the weak-link regime of BSG could be discovered by the *d*of the gels. For example, protein gels take values primarily between 1.5 and 2.8 as reported [10].

In recent times, the gelation and fractal dimension of fibrin gel prepared by iron oxide nanoparticles were performed [11]. Muthukumar's theory was applied for calculating of fractal dimensions of nanocomposites. The values of them were as 1.61 and 1.69 with low and high contents of thrombin. XRD and XPS were used in the structural and fractal analysis of terbium acetate (Tb^{+3}) doped ZnO nanoparticles [12]. Its fractal dimension was calculated from height- height correlation function which was increased by dopant material. Indeed, fractal dimension and gelation behavior of ovalbumin (OVA) prepared by various carboxymethylcellulose (CMC) were mentioned [13]. When increasing CMC, the gel strength was increased in the electrostatic complexes. Their fractal dimensions were found from 1.83 to 1.75 for OVA/CMC 0.7 with transition regime. On the other hand, the viscoelasticity, fractal dimension and gelation properties of the galactomamans were studied [14]. The sol- gel mechanism has been tested by dynamic rhelogical tests. And also, the fractal dimensions of them were modeled with Shih's and Morbidelli's theories. They were 1.82 using Shih model whereas they were 2.38 using Morbidelli's model for fenugreek gum (FG). In a new study, there is a correlation between fractal analysis and nanograin growth [15]. Therefore, $BaTiO_3$ thin film was prepared and their ferroelectric morphology, grain size and fractal dimensions were analyzed. When self-similarity of them decreases, their fractal dimensions decrease. Moreover, research has shown that if PAAm was fabricated by zeolite, its water vapor adsorption capacity was decreased with increasing temperature [16]. When it was prepared in the presence of nanorods [17], they can be used to minimize secondary waste in the environment. In our group, the fractal dimensions of PAAm -GO composites were studied [18] by Fluorescence spectroscopy. The correlation between gelation and fractal dimension was found. Thus, the dimension was found as 2.63 at 25 min.

In this study, photon transmission was used to observe AAm copolymerization, altering Bis contents, *BC*. The gelation activity caused the photons transmitted to be much less intense (lower I_{tr}), and the light scattered from the gel was more intense (higher I_{sc}), which may indicate spatial phase separation while AAm with Bis was being copolymerized. The increase in I_{sc} as opposed to the Bis content was used to calculate the fractal dimension, d, assuming that there was a linearity of the expanding volume of microgel particles and the time variable and a proportionality of the quantit y of particle concentration to the Bis content in the cross-linked PAAm gel. It is understood that self-similarity among gels is strictly controlled by the Bis content in the gel. Evaluations of the fractal dimension, d versus gelation and swelling time were studied during the gelation and swelling processes of acrylamide gels, where scattering intensity experiments were employed to produce d values in both processes. In the process of gelation, the fractal dimension rose to 3.00 from the deep with higher gelation time, presenting $d = 2.57$ for the percolation cluster at the intermediate time. Similarly, the fractal dimension during swelling was raised up to 1.66 from 1.00 as the swelling time increased, predicting Dragon curve type channels in the swollen PAAm gel. Thus, the evaluation of fractal dimension of PAAm during gelation and swelling process was performed to detect the structural changes.

2. Experimental

For PAAm gels, the monomer AAm (Acrylamide, 110,784 Merck, Germany) by 2.5 g was used together with an initiator, APS (ammonium per sulfate, A6761 Sigma-Aldrich, Germany) by 40 mg. Bis (N,N′ -methylenebis(acrylamide), 146,072 Sigma-Aldrich, Germany) was used as crosslinking agent, and 10 μl of TEMED (tetramethylethylenediamine, T22500 Sigma-Aldrich, Germany) as an accelerator in FCC process. These components were dissolved in distilled water (25 mL) to produce eight different gels. The crosslinker (Bis), was mixed into individual sols in different Bis content, *BC* (50, 100, 125, 150, 175, 200, 250 and 300 mg) during the sample preparation process by a previously provided recipe [19]. The temperature was under room conditions for each process, and 1.0×1.0 cm^2 quartz cells in air were placed in a Perkin-Elmer UVV spectrometer for in situ experiments of photon transmission to monitor the gelation processes periodically. The time drive mode, as well as the wavelength of 690 nm, was selected on the device to follow up photon transmission intensities, I_{tr} within the period of copolymerization of AAm. The reason for choosing this wavelength is that transmission and scattering graphics give the best appearance without being completely saturated.

Seven different 1 cm diameter cylindrical samples prepared according to the recipe used in previous gelation experiments were cut into 5 mm thick discs and then dried to a thickness of 1.4–1.6 mm. The swelling experiments were started by placing them in water-filled quartz reservoirs and experiments were carried out with UVV spectrometer [20]. The monitoring phase was followed again for swelling of the gels to record in situ photon transmission values with the use of the Perkin–Elmer UVV spectrometer. Similar to the case of gelation, 440 nm was preferred for these measurements because of the graphical appearance and to obtain curves that are not saturated and that can be distinguished properly. In both cases, after each measurement, transmission intensity was converted to scattering intensity based on the relation $I_{sc} = 1 - I_{tr}$, for fractal analysis of gelation and swelling measurements. Thus, I_{sc} refers to the structural fractal-like heterogeneities for gelation and swelling processes of PAAm gel.

3. Results and discussion

3.1. Gelation

Raw experimental I_{tr} data for the samples containing eight different amounts of Bis content, *BC* are shown in Fig. 1 [19]. Here, the decreases in the I_{tr} curves, in other words the increases in I_{sc}, are due to the gelation

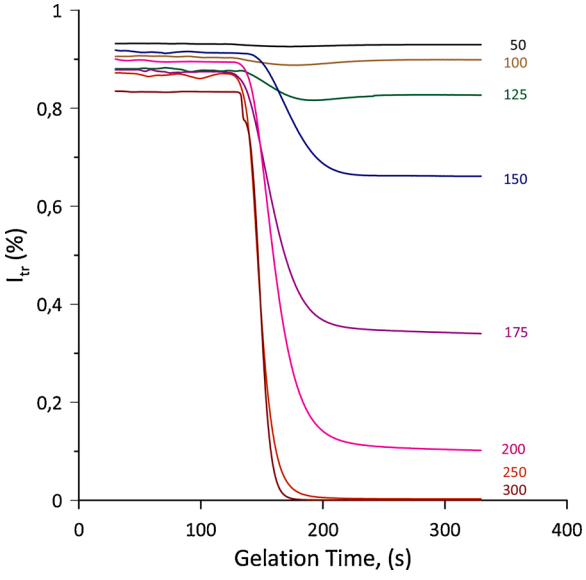

Fig. 1. Variation in transmitted photon intensities, I_{tr} versus gelation time for eight different Bis content, *BC*. Numbers on each curve present the *BC* in milligrams.

reaction that started about 120 s after the accelerator was added. It is clearly seen that the increase in the *BC* amount causes a dramatically increased scattering in the gelled samples. Because the increase in the amount of crosslinker causes the fractal-like structure formed to become more complex. In other words, it causes an increase in the heterogeneity and consequently the scattered light intensity, I_{sc}.

The normalized I_{sc} curves corresponding to Bis contents were related to the FCC in six different gelation times (125, 150, 175, 200, 225 and 250) in seconds. The curves for 175 s and 250 s are shown in Fig. 2. Fig. 2 displays that the I_{sc} value increased on levels much higher than a specified Bis content, *BC* meaning that heterogeneities occurred during gelation, potentially with opalescence. In this study, greater light scattering due to hydrogel system indicated a strong opalescence higher than such a critical value. Modeling results depend on the occurrence that PAAm microgels are formed till the macrogelation phase [21]. Further with the reaction, pendant vinyls and radical ends on the periphery of microgels make them bound to a macrogel. Thereby, the junction points are identified as highly intramolecular cross-linked microgel particles that are created prior to completion of gelation. Accordingly, these particles can be judged as the junction points of the final structure including heterogeneities. Greater content of the cross-linker expands the microgel with higher compactness and/or concentration of the junction points when the inter-microgel distance remains the same [22]. It can be seen from the curves in Fig. 2 that when using 0.3 g *BC*, the percent of light scattered from the structure is 1, indicating that the structure is completely heterogeneous and consists entirely of microgels. Therefore, *BC* values can be normalized by assuming the 0.3 value of *BC* as a maximum (BC^{max}). For the cross-linked PAAm gel, the proportionality of the concentration of microgel particles to the Bis content may produce the following relation of the scattering intensity and Bis content [4,5]

$$I_{sc} = (BC_{norm})^{d} \tag{1}$$

where d is the fractal dimension which is a decisive parameter for measuring the internal structure of the gel, during the variation of normalized Bis content ($BC_{norm}=BC\ /\ BC^{max}$) which determines the structural variations in the growing and swelling gel.

Here, Eq. (1) is produced from well-established arguments for self-similar object, such as Perimeter of Koch Curve, Snow Flake, Sierspinski Gasket and Carpet, Menger Sponge and Percolation Clusters etc. All possess Fractal like structure, which obey the relation given below [1,23,24]

$$N = M^{d} \tag{2}$$

Eq.(2) is produced from standard self-similarity, where M is the number of resolution and N is the number of pieces under this resolution. Here d represents Fractal dimension for self-similar object and dimension for Euclidian structures. In Eq.(1) since normalized Bis content, BC_{norm} presents the number of microgel particles in the medium, it can be taken as an analogy to number of resolution in Eq.(2). Similarly, Since I_{sc} is proportional to number of heterogeneity in the medium, then it can be taken as the number of pieces under micro gel resolution. Eventually, d in Eq.(1) can be named as Fractal dimension for the system under investigation. Under these assumptions, Eq. (1) can also be interpreted, by knowing the fact that light scattering is caused by density and concentration fluctuations, i.e. by deviation of density and concentration from their uniform values in a dispersed medium. Light is scattered only when a light wavelength, λ, is greater than the size of a particle of the dispersed phase. If λ is much smaller than the particle diameter, light is reflected. Rayleigh derived an equation by excluding the absorption of light by the medium, which connects I_0 with I_{sc}, the intensity of light scattered per unit volume of a dilute system as follows:

$$I_{sc} = I_0 \kappa c \nu^2 \lambda^{-\eta} \tag{3}$$

This equation is valid for particles which are small in comparison with the wavelength λ of the incident light. In Eq. (3) κ contains the indices of refraction of the dispersed phase and the dispersion medium. ν represents the volume of a single particle and c is the concentration of particles of the system in Eq. (3). Rayleigh's equation determines the opalescence of the medium and can be used for particles whose size is not more than 0.1 of the wavelength of light, i.e. for particles of diameters from 40 to 70 nm. In this case, I_{sc} changes in inverse proportion to the fourth power of λ. When the size of the particles in the dispersed medium becomes much greater than λ, light is no longer scattered but reflected, regardless of the wavelength of the incident light. In Eq. (1), it is assumed that BC_{norm} is proportional to c in Eq. (3), where the other parameters are assumed to be constants of a given medium, and given time, here BC_{norm} is chosen as a parameter to design the structural changes, resulting to produce the fractal dimension during gelation and swelling processes. In Fig. 3(a) and (b), the Log-Log plots present normalized I_{sc} values versus the normalized Bis content (BC_{norm}) for different gelation times, where d values are computed using the slope of each linear curve. Additionally, Fig. 4 shows the plot of these estimates of the fractal dimension versus the gelation time, representing their association. The 150-second gelation process produced a d value of 1.87,

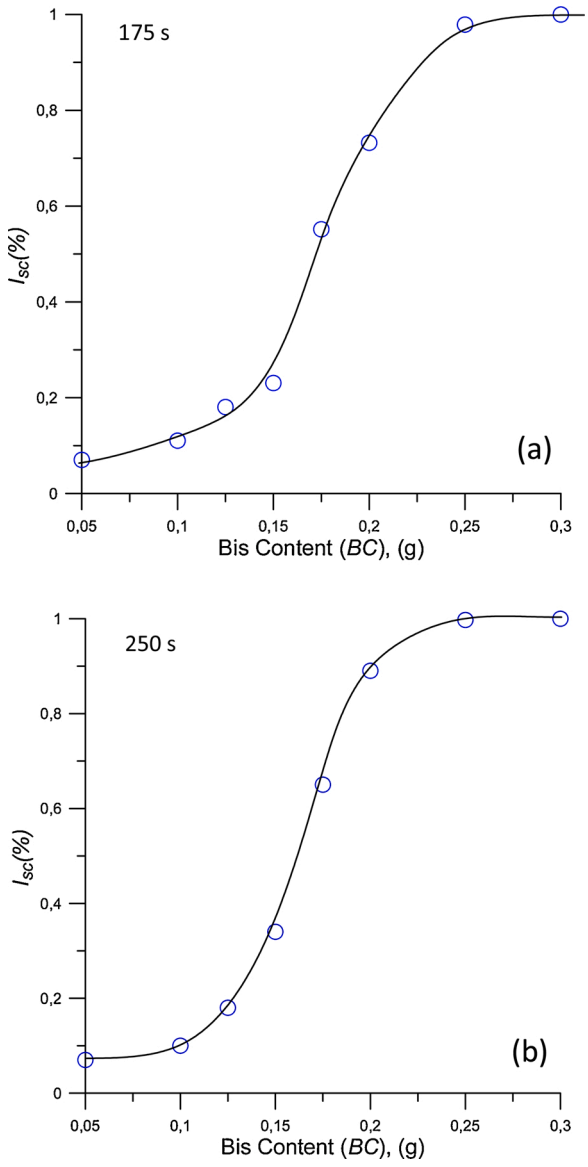

Fig. 2. The plots of the scattered photon intensities, I_{sc} versus the Bis content, *BC* values at various gelation times a) 175 s, and b) 250 s.

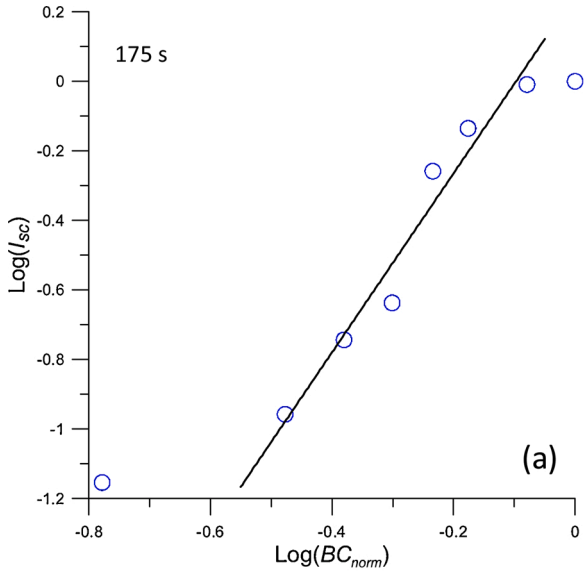

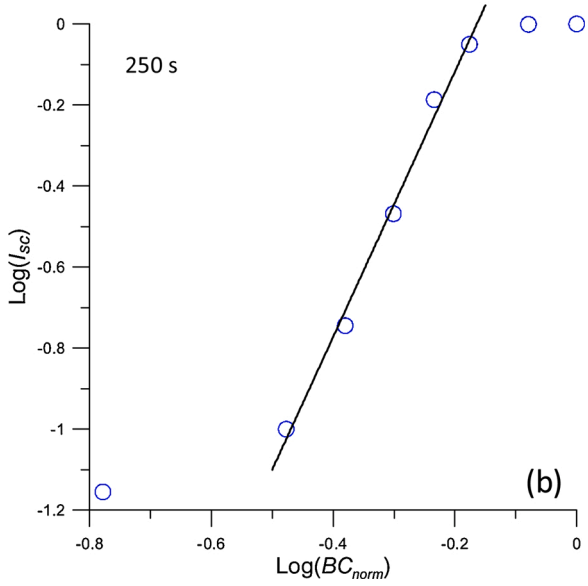

Fig. 3. Log-Log plots of I_{sc} versus (BC_{norm}) and their fits to Eq. 1 for various gelation times a) 175 s, and b) 250 s. Here, the slopes of the linear relations produce fractal dimensions at given gelation times.

potentially corresponding to a fractal percolation with 75 % probability [22] and/or can be speculated to the von Koch curve and the Cantor set [22] The fractal dimension 2.57 at 175 s, with no doubt, was nearly the same as a 3D percolation cluster with a d value of 2.52 [25,26]. Longer than 200 s the PAAm gel approached 3-dimensional networks as expected.

3.2. Swelling

Fig. 5 shows the raw I_{tr} – swelling time curves of the swelling experiments with initially dried seven different Bis content, BC gels. At the beginning of the swelling process, a rapid increase in I_{tr} values is observed. The transmitted light intensity, I_{tr} then decreases during the actual swelling process and I_{sc} increases accordingly. The reason for the initial rise can be explained as follows: Possible micro cracks and structural defects on the surface due to the cutting of gels cause excessive light scattering on the dry gel surface, then the gel surface becomes

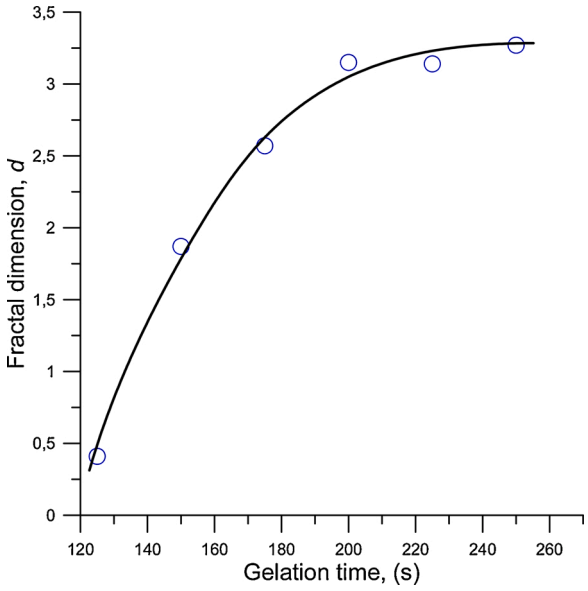

Fig. 4. The plot of the fractal dimension, d versus the gelation time.

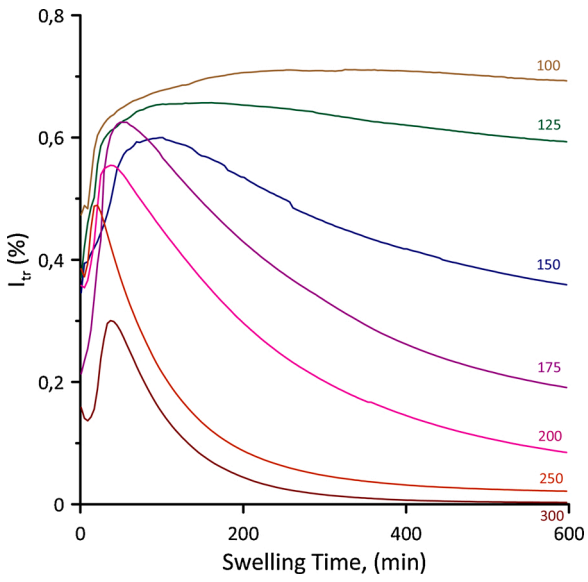

Fig. 5. Variation in transmitted photon intensities, I_{tr} versus swelling time during swelling process for different Bis content, BC samples. Numbers on each curve present the Bis content, BC in milligrams.

smoother when wet for 50−100 min (min). This behavior of I_{tr} can also be named as the surface effect related to the dangling chain ends, which cause some scattering from the gel surfaces before wetting. It is well known that a "frozen blob" appears where two junctions are positioned on adjacent lattice sites [2]. The higher quality of solvent swells the gel to expand frozen blob clusters up to less than the interstitial medium. For swollen gels, low concentration areas could be created with removal of small ones from bigger clusters. In this study, the typical size of non-entangled clusters with smaller ones was described as the correlation length. Namely, the size is referred to as that of the holes that appear as a part of the interstitial medium. Afterwards, being swollen allows for light to excessively scatter due to the contrast between frozen blob clusters and holes caused by dilution. Dilution partially separates frozen blob clusters during gel swelling, which dramatically increases the scattering intensity, I_{sc}. Swollen gels contain inseparably bound cross-links due to the chemical property of a chain segment which is at

an optimal excluded volume conformation. The mostly connected frozen blobs form clusters of first topological neighbors so that a site percolation on a blob lattice may be identified from the random cross-linking of chains [2]. Fig. 6 presents the results of I_{sc} obtained from the swelling gels against the Bis content at 200 min and 500 min of swelling times. It is seen that higher *BC* values escalated light scattering from the swelling gel for all the applied times. Eq. (1) gives variations in the fractal dimension throughout the swelling processes. Here, each frozen blob assumingly corresponds to an individual microgel available on the PAAm system. Here too, in order to obtain normalized *BC* numbers, a normalization similar to that in the gelation case can be applied using a maximum value of 0.3 g *BC* where percent of I_{sc} is 1. The Log-Log plots of I_{sc} versus normalized Bis content, (BC_{norm}) are given in Fig. 7(a) and (b), from where the slope of the curves produces the fractal dimensions *d*, which is plotted in Fig. 8. It may be seen that, at 100 min as the gel just starts to swell, the fractal dimension (1.17) is almost 1.0, suggesting that water molecules enter into the linear tubes, and as the swelling time increases, these tubes start curving, and as a result of this, the fractal dimension increases from 1.3 to 1.53 to eventually 1.66. Here, the end of the swelling water molecule follows the roads of Dragon curves with the

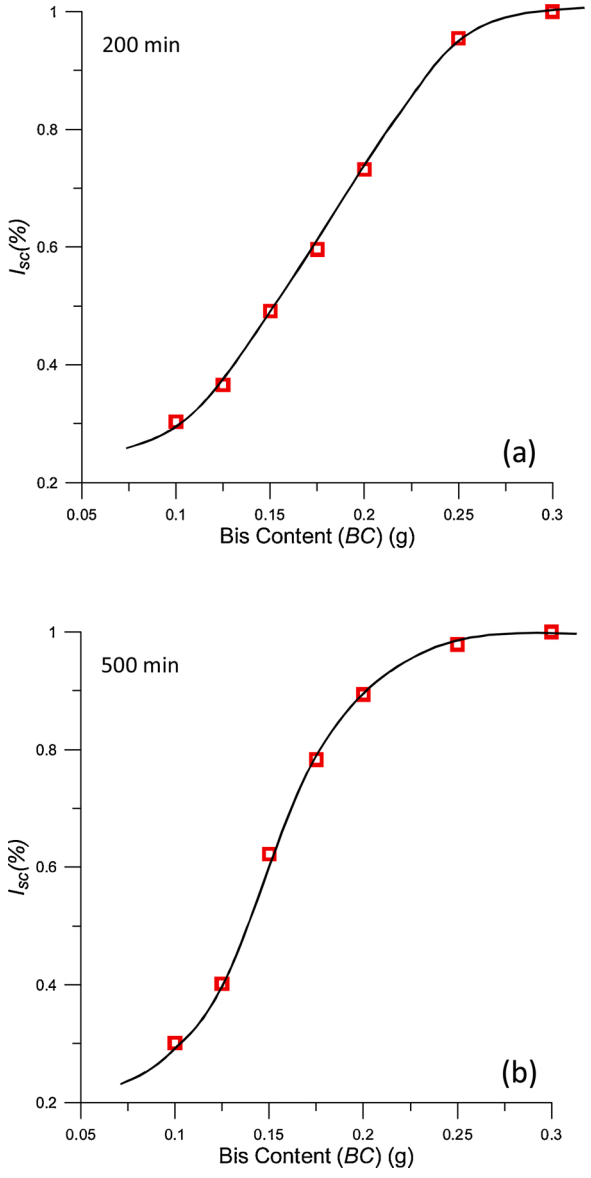

Fig. 6. The plots of the scattered photon intensities, I_{sc} versus the Bis content, *BC* values at various swelling times a) 200 s, and b) 500 s.

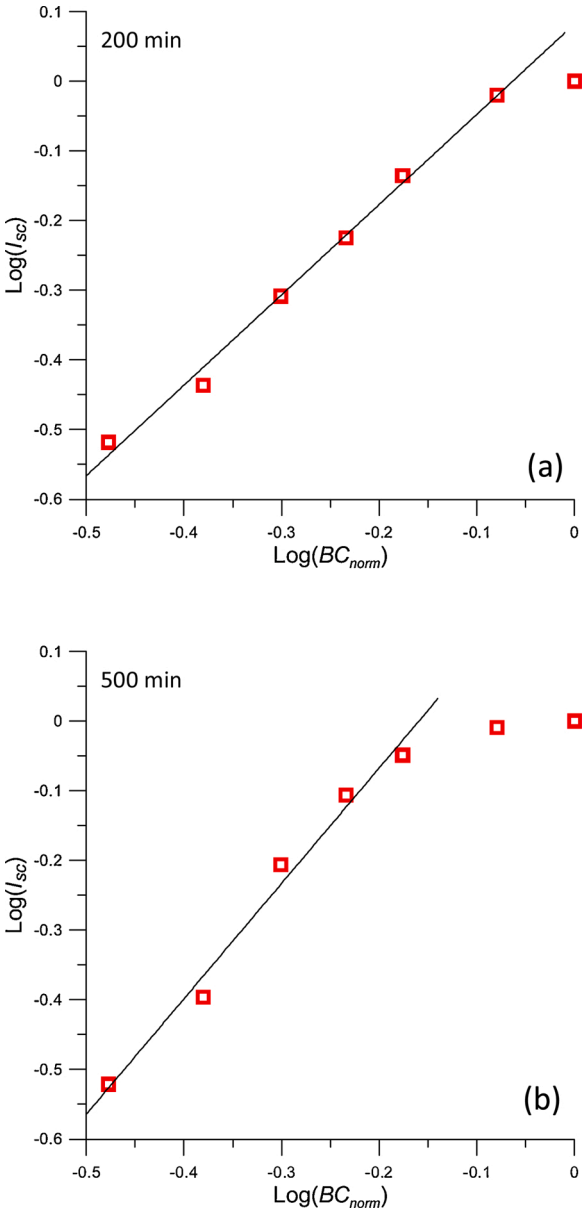

Fig. 7. Log-Log plots of I_{sc} versus (BC_{norm}) and their fits to Eq. 1 for various swelling times a) 200 s, and b) 500 s. Here, the slopes of the linear relations produce fractal dimensions at given swelling times.

dimension of 1.618 [23,24].

4. Conclusions

This study reports a photon transmission experiment within the process of copolymerization of AAm by varying Bis content, *BC* and swelling of these gels. Lower intensity, I_{tr} of the transmitted photon was observed along with the gelation and swelling processes. This result may account for the higher intensity of the scattered light, I_{sc} from the gel depending on the spatial phase separation occurring throughout copolymerization of AAm with Bis and swelling. The increasing I_{sc} values during gelation corresponding to the normalized Bis content, BC_{norm} were used to calculate the fractal dimension, *d*. In our study, this was found to increase from very low values to 3.00 by the increase in gelation time, presenting $d = 2.57$ for the percolation cluster at the intermediate time. Similarly, the fractal dimension during swelling was found to increase from 1.00 to 1.66 with longer swelling time periods, predicting that, at the end of the swelling process, the gel formed Dragon

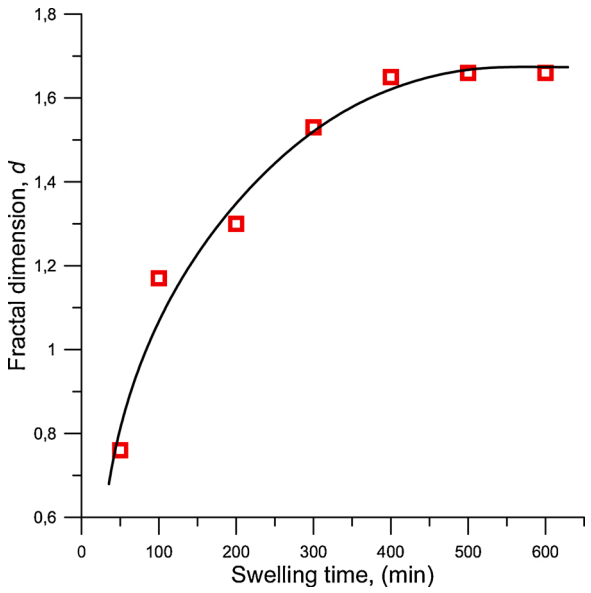

Fig. 8. The plot of the fractal dimension, *d* versus the swelling time.

curve type channels in the swollen PAAm gel. In conclusion, these new findings provide the fractal analysis produced important parameters related to structural changes during gelation and swelling processes.

Declaration of Competing Interest

The authors declare that they have no known competing financial interests or personal relationships that could have appeared to influence the work reported in this paper.

References

[1] P. Pfeifer, in: L. Pietronero, E. Tosatti (Eds.), Fractals in Physics, Elsevier Science Publishers, B.V, Amsterdam, 1986, pp. 47–53.
[2] J. Bastide, L. Leibler, Large-scale heterogeneities in randomly cross-linked networks, Macromolecules 21 (8) (1988) 2647–2649.
[3] K. Dusek, Polymer Networks Structure and Mechanical Properties, Plenum Press, New York, 1971.
[4] J. Bastide, L. Leibler, J. Prost, Scattering by deformed swollen gels-butterfly isointensity patterns, Macromolecules 23 (1990) 1821–1825.
[5] J.E. Martin, A.J. Hurd, Scattering from fractals, J. Appl. Crystallogr. 20 (1987) 61–78.
[6] Y. Yılmaz, A. Erzan, Ö. Pekcan, Critical exponents and fractal dimension at the sol-gel phase transition via in situ fluorescence experiments, Phys. Rev. E 58 (1998) 7487–7491.
[7] C.-H. Bi, D. Li, L.-J. Wang, B. Adhikari, Viscoelastic properties and fractal analysis of acid-induced SPI gels at different ionic strength, Carbohydr. Polym. 92 (2013) 98–105.
[8] Y. Wang, D. Li, L-j. Wang, Wu, M.N. Özkan, Rheological Study and Fractal Analysis of Flaxseed Gum Gels, Carbohydr. Polym. 86 (2011) 594–599.
[9] D.Q. Yuan, Y.L. Wang, J. Feng, Contribution of stratified extracellular polymeric substances to the gel-like and fractal structures of activated sludge, Water Res. 56 (2014) 56–65.
[10] A. Rafe, S.M.A. Razavi, Scaling Law, Fractal analysis and rheological characteristics of physical gels cross-linked with sodium trimetaphosphate, Food Hydrocoll. 62 (2017) 58–65.
[11] M.N. Kirichenko, L.L. Chaikov, S.V. Krivokhizha, A.S. Kirichenko, N.A. Bulychev, M.A. Kazaryan, Effect of iron oxide nanoparticles on fibrin gel formation and its fractal dimension, J. Chem. Phys. 150 (1–8) (2019) 155103.
[12] A. Kumar, A. Sharma, S. Bhasker, R.P. Yadav, H.P. Bhasker, P.K. Priya, K. L. Pandey, S.K. Mandal, R.K. Anand, Study of structural and surface morphological properties of Tb doped ZnO nanoparticles using XRD, XPS and fractal analysis, Mater. Res. Express 6 (1–10) (2019) 115039.
[13] W. Xiong, C. Ren, X. Xu, J. Li, L. Wang, B. Li, Thermally induced gelation behavior and fractal analysis of ovalbumincarboxymethylcellulose electrostatic complexes, Food Hydrocoll. 91 (2019) 214–223.
[14] P.V. Gadkari, M.J.T. Reaney, S. Ghosh, Assessment of gelation behaviour of fenugreek gum and other galactomannans by dynamic viscoelasticity, fractal analysis and temperature cycle, Int. J. Biol. Macromol. 126 (2019) 337–344.
[15] H. Aminirastabi, H. Xue, V.V. Miti, G. Lazovi, G. Ji, D. Peng, Novel fractal analysis of nanograin growth in $BaTiO_3$ thin film, Mater. Chem. Phys. 239 (1–10) (2020) 122261.
[16] H. Mittal, A. Al Alili, S.M. Alhassan, Adsorption isotherm and kinetics of water vapors on novel superporous hydrogel composites, Microporous Mesoporous Mater. 299 (1–13) (2020) 110106.
[17] N. Kumar, H. Mittal, S.M. Alhassan, S.S. Ray, Bionanocomposite hydrogel for the adsorption of Dye and reusability of generated waste for the photodegradation of ciprofloxacin: a demonstration of the circularity concept for water purification, ACS Sustain. Chem. Eng. 6 (2018) 17011–17025.
[18] G. Akın Evingür, Ö. Pekcan, Fractal dimension and phase transition of graphene oxide (GO) doped polyacrylamide, Polym. Test. 84 (1–5) (2020) 106386.
[19] S. Kara, Ö. Pekcan, Photon transmission technique for monitoring free radical crosslinking copolymerization in various crosslinker contents, Polymer 41 (8) (2000) 3093–3097.
[20] Ö. Pekcan, S. Kara, Lattice heterogeneities at various crosslinker contents—a gel swelling study, Polymer 41 (24) (2000) 8735–8739.
[21] H.J. Naghash, O. Okay, Formation and structure of polyacrylamide gels, J. Appl. Polym. Sci. 60 (7) (1996) 971–979.
[22] K. Falconer Fractal Geometry: Mathematical Foundations and Applications John Wiley& Sons Ltd., New York (1990-2003).
[23] B.B. Mandelbrot, The Fractal Geometry of Nature, W.H. Freeman and Co, New York, 1983.
[24] S. Kara, E. Arda, Ö. Pekcan, Fractal dimensions of κ-Carrageenan gels during gelation and swelling, J. Macromol. Sci. Part B- Phys. 57 (11–12) (2018) 715–773.
[25] M. Sahimi, Applications of Percolation Theory, CRC Press, 2003.
[26] D. Stauffer, A. Aharony, Introduction to Percolation Theory, 2 ed, Taylor and Francis, London, 1994.